Science of the Total Environment 756 (2021) 143726

Contents lists available at ScienceDirect

Science of the Total Environment

journal homepage: www.elsevier.com/locate/scitotenv

A systematic comparison of commercially produced struvite: Quantities, qualities and soil-maize phosphorus availability

Maarten Muys [a], Rishav Phukan [a], Günter Brader [d], Abdul Samad [d], Michele Moretti [a], Barbara Haiden [b], Sylvain Pluchon [c], Kees Roest [e], Siegfried E. Vlaeminck [a,*], Marc Spiller [a]

[a] Research Group of Sustainable Energy, Air and Water Technology, Department of Bioscience Engineering, University of Antwerp, Groenenborgerlaan 171, 2020 Antwerpen, Belgium
[b] Timac AGRO Düngemittelproduktions- und Handels Gmbh, Industriegelände Pischelsdorf, 3435 Zwentendorf, Austria
[c] Centre Mondial de l'Innovation Roullier - Laboratoire de Nutrition Végétale, 18 avenue Franklin Roosevelt, 35400 Saint-Malo, France
[d] AIT Austrian Institute of Technology GmbH, Bioresources Unit, Konrad-Lorenz-Strasse 24, 3430 Tulln, Austria
[e] KWR Water Research Institute, Groningenhaven 7, 3433 PE Nieuwegein, the Netherlands

HIGHLIGHTS

- Struvite from 30% of the 80 worldwide installations were analyzed in detail.
- All but three struvite samples meet all EU fertilizer directive standards.
- Struvite granule size and shape highly depend on substrate type to recover from.
- P availability and plant biomass yields were similar across struvite samples.
- Current struvite production is limited, demonstrating large potential for growth.

GRAPHICAL ABSTRACT

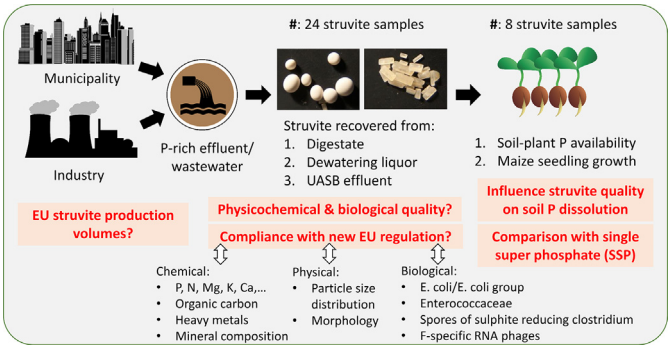

ARTICLE INFO

Article history:
Received 3 September 2020
Received in revised form 29 October 2020
Accepted 10 November 2020
Available online 24 November 2020

Editor: Yifeng Zhang

Keywords:
Magnesium ammonium phosphate
Nutrient recovery
Phosphorus recovery
Bio-based fertilizers
Struvite characterization
Circular economy

ABSTRACT

Production of struvite ($MgNH_4PO_4 \cdot 6H_2O$) from waste streams is increasingly implemented to recover phosphorus (P), which is listed as a critical raw material in the European Union (EU). To facilitate EU-wide trade of P-containing secondary raw materials such as struvite, the EU issued a revised fertilizer regulation in 2019. A comprehensive overview of the supply of struvite and its quality is presently missing. This study aimed: i) to determine the current EU struvite production volumes, ii) to evaluate all legislated physicochemical characteristics and pathogen content of European struvite against newly set regulatory limits, and iii) to compare not-regulated struvite characteristics. It is estimated that in 2020, between 990 and 1250 ton P are recovered as struvite in the EU. Struvite from 24 European production plants, accounting for 30% of the 80 struvite installations worldwide was sampled. Three samples failed the physicochemical legal limits; one had a P content of <7% and three exceeded the organic carbon content of 3% dry weight (DW). Mineralogical analysis revealed that six samples had a struvite content of 80–90% DW, and 13 samples a content of >90% DW. All samples showed a heavy metal content below the legal limits. Microbiological analyses indicated that struvite may exceed certain legal limits. Differences in morphology and particle size distribution were observed for struvite sourced from digestate (rod shaped; transparent; 82 mass% < 1 mm), dewatering liquor (spherical; opaque; 65 mass% 1–2 mm) and effluent from upflow anaerobic sludge blanket reactor processing potato wastewater (spherical; opaque; 51 mass% < 1 mm and 34 mass% > 2

* Corresponding author.
E-mail address: siegfried.vlaeminck@uantwerpen.be (S.E. Vlaeminck).

https://doi.org/10.1016/j.scitotenv.2020.143726
0048-9697/© 2020 The Authors. Published by Elsevier B.V. This is an open access article under the CC BY license (http://creativecommons.org/licenses/by/4.0/).

mm). A uniform soil-plant P-availability pattern of 3.5–6.5 mg P/L soil/d over a 28 days sampling period was observed. No differences for plant biomass yield were observed. In conclusion, the results highlight the suitability of most struvite to enter the EU fertilizer market.

© 2020 The Authors. Published by Elsevier B.V. This is an open access article under the CC BY license (http://creativecommons.org/licenses/by/4.0/).

1. Introduction

Phosphorus (P) is an essential macronutrient for all living organisms, classified as a critical raw material by the European Commission (EC, 2020). About 90% of commercially available P is sourced from phosphate rock, a non-renewable and geographically restricted resource, with no meaningful reserves in the European Union (EU) (Chowdhury et al., 2017). To counter resource dependency and to realize sustainable P management, implementing P recovery is imperative. In society, the largest P losses occur through domestic wastewater (15% of total EU import) (van Dijk et al., 2016). In this regard, P recovery through struvite precipitation from wastewater ($MgNH_4PO_4.6H_2O$) has received much attention. The reasons for this are that struvite has a theoretical P content close to that of phosphate rock (12.6% dry weight (DW)), it has been demonstrated to be an effective P fertilizer especially in acidic soils, and it is considered a slow release fertilizer that can reduce P losses to the environment (Everaert et al., 2018; Hertzberger et al., 2020). Furthermore, our research shows that struvite is currently mainly marketed at values between €0–100 per ton, but also at considerably higher prices of €350 per ton (Phoshorgreen) to €1000 (Pearl) per ton. This implies that in about 80–87% of the cases struvite is sold at lower prices than the estimated market value of its macro nutrients, namely €250–412 per ton (first value: literature De Vrieze et al. (2019) assuming €1900 t P fertilizer; own calculations: €549 t urea 47% N and 5.7% N in struvite and the value of €233 t single super phosphate (SSP) at 7.7% P – at farm price in Austria September 2020 excl. VAT -personal communication Timac AGRO). Finally, struvite production technologies have matured since their first application (Egle et al., 2016). Shaddel et al. (2019) identified 80 struvite producing plants world-wide, operating 19 different technologies. Three basic types of struvite precipitation processes can be distinguished (Fig. 1). Type I receives waste activated sludge (WAS and primary sludge if applicable) and/or digestate originating from anaerobic digestion (AD) in continuous stirred tank type reactors (CSTR). Type II struvite is precipitated on the dewatering liquor of the WAS digestate after a solid-liquid separation step (e.g. centrifugation). A key difference between the two streams is the lower total suspended solids (TSS) content in the influent to the struvite reactor (e.g. 21–28 g TSS/L digestate vs.0.9–1 g TSS/L dewatering liquor, as measured in this study). In several cases, type II struvite reactors also receive a P-rich liquor from WAS thickening prior to anaerobic digestion (Fig. 1). Type III struvite is sourced from agro-industrial wastewater treatment (i.e. potato processing, dairy). The main application is the potato industry (Abma et al., 2010; Moerman et al., 2009); in these applications struvite is precipitated directly from the liquid effluent of anaerobic digestion in upflow anaerobic sludge blanket (UASB) reactors. These liquid effluents typically are relatively low in TSS content (e.g. 0.5 g TSS/L) (Muys et al., 2020).

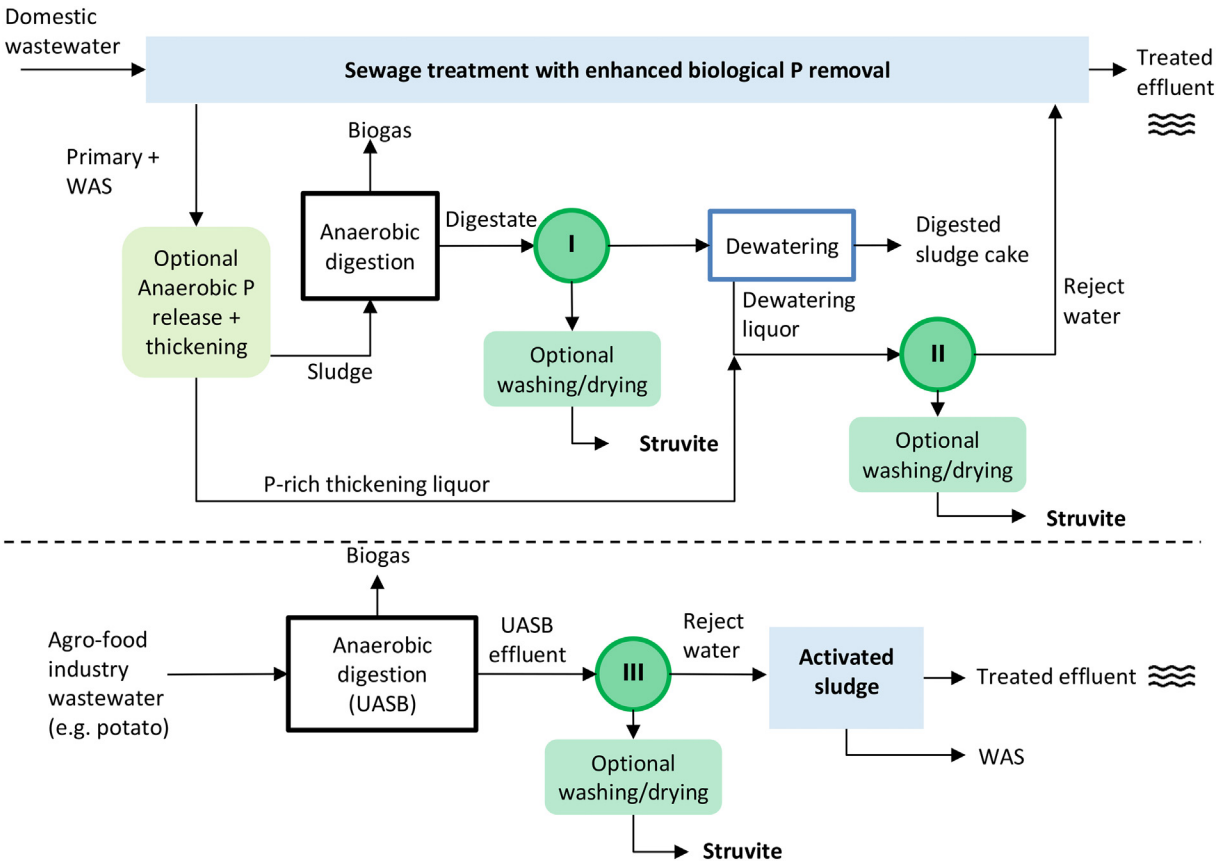

Fig. 1. Three categories in which struvite recovery processes in Europe can be classified. Depending on the type of water/slurry and location of the struvite recovery process in a wastewater treatment plant (WWTP) I: on digestate of sewage waste activated sludge (WAS); II: on the dewatering liquor of sewage WAS digestate; III): after anaerobic digestion of agro-industrial wastewater. (UASB: upflow anaerobic sludge blanket).

The different influent types and technologies implemented may affect struvite quality as struvite crystallization is governed by several interacting parameters including, amongst others, influent P concentration, crystal retention time, TSS concentration, viscosity, presence of colloidal substance, Mg:P ratio, pH and mixing conditions (Doyle and Parsons, 2002). As a result, the produced struvite is likely to vary in crystal size, presence of co-precipitates and inclusion of organics and other contaminants. However, currently there is no systematic comparison of struvite quality from different full-scale installations. Yet, such an analysis is imperative in the context of the recent publication of the new European fertilizer regulation that is setting EU-wide quality standards for struvite and hereby facilitating its EU-wide trade (EC, 2019).

The new fertilizer regulation defines 17 physicochemical and 5 microbiological parameters that struvite should meet to be utilized as a fertilizer or component material in N-P-K fertilizers (supplemental material (SM), Table S1). In addition to the regulation, it is proposed that physical parameters and the solubilization rate of struvite are critical for further commercial use of struvite (Huygens et al., 2017). Struvite granules must be of a shape and size which enable its utilization in modern application equipment or allow blending with N and K containing granules (Spiller et al., 2019). Alternatively, struvite with very small and heterogeneous granules may be more suitable for application in growing media or can be re-processed into an N-P-K fertilizer (Grunert et al., 2019; Spiller et al., 2019). Furthermore, it is known that struvite is not purely comprised of $MgNH_4PO_4.6H_2O$, but does contain other precipitates (e.g. brushite, dittmarite, amorphous components). These precipitates do not only have a different N and P content, but also have different solubilization characteristics. Furthermore, it was shown that plants influence struvite P solubility through producing exudates (e.g. organic acids) and that therefore an investigation of P solubilization for the system comprising plant and soil is required (Talboys et al., 2016).

Answering to the knowledge gaps outlined, this study had three objectives. Firstly, to estimate the current EU struvite production volumes. Secondly, to compare the physicochemical and microbiological characteristics of struvite samples from 24 installations across the EU and to evaluate them against the new European fertilizer regulation. Thirdly, to provide insights on parameters not regulated for, that are known to affect utilization and fertilization characteristics of struvite, including mineralogical composition, particle size distribution and to study soil-plant P-availability and the fertilization performance.

2. Methodology

2.1.1. Struvite sampling

In this study, information about all known full-scale struvite installations was gathered through literature review, industrial contacts, web search and interaction at international conferences. In total 39 operational installations were identified (source separated decentralized installations were excluded, Table S2, SM Section 4) and 25 struvite samples were collected from 24 different installations across Europe (Table 1). All but one sample were collected in the period 2018–2019. For every sample collected, process engineers and technical staff were interviewed to gain insight into operational conditions of the struvite precipitation process. The samples are classified into the three main struvite recovery categories introduced above.

2.2. Physicochemical struvite characterization

Before the physicochemical analyses, all samples were oven dried, the drying was performed at a temperature of 40 °C (Huygens et al., 2017). Subsequently, samples where further prepared for the different analyses as described in the SM Section 3. Phosphorus was extracted according the EC, 2003/2003 method 3 and 3.1.1 (EC, 2003) and measured according the spectrophotometric vanadomolybdate method (APHA et al., 2012). Ammonium was analyzed using the Kjeldahl method (SM Section 3). For the total organic carbon (TOC) analysis, the struvite was dissolved in distilled water and determined using an online TOC-V series Shimadzu analyzer (TOC-VCPH autosampler ASI). Heavy metals and cations were analyzed using Inductively Coupled Plasma – optical emission spectrometry (ICP-OES; 5110 VDV Agilent Technologies, USA). Potassium and magnesium were extracted according the standardized method EC, 2003/2003 method 4.1 and 8.1 (EC, 2003). Struvite bulk mineralogical composition was measured by X-ray diffraction (XRD; using CuKα radiation; Bruker D8 Advance diffractometer and PDF-4 crystal structure database of the International Centre for Diffraction Data). A mass balance was constructed integrating data from the different analysis outlined above (SM Fig. S1). Struvite content was estimated using both the mineralogical data from the XRD and data on the elemental composition (SM Fig. S1). A particle size distribution (PSD) of all struvite samples was made using sieve analysis (mesh sizes of 200, 500, 1000, 1600, 2000, 2500, 3150, 3550 and 4500 μm) (norme Française; European norm, NF EN 1235).

2.3. Microbiological struvite characterization

Pathogenic microorganisms were determined for three fresh samples of Airprex 1, Pearl 1 and NuReSys 4 (Table 1). To explore the effect of storage on pathogen contamination the samples of Airprex 1 and Phosgreen 2 were kept for 9 months at room temperature in the dark. To determine the distribution of pathogens between struvite crystals and impurities, the visible debris of the fresh Airprex 1 was removed manually before a second pathogen analysis was performed.

The STRUBIAS document sets limits for selected pathogens, e.g. *Salmonella* spp., *E. coli* or *Enterococcaceae*, *Clostridium perfringens*, *Ascaris* sp. (Huygens et al., 2017) (Table S1 SM). The pathogens analyzed in this study deviate from the STRUBIAS indicators in that no analysis of *Salmonella* was performed and that the analysis of spores of sulphide reducing clostridia (SSRC) is used as an indicator for C. *perfrigens*, *Ascaris* sp. eggs and *Cryptosporidium* oocysts due to their persistence to wastewater treatment processes (Guzman et al., 2007). Furthermore, F-specific RNA phages were used as an indicator for enteric viruses (Guzman et al., 2007). These analytical approaches were followed because defined methodological procedures were not available at the time of the study and no laboratories were available to analyze the required parameters.

For all biological contaminants, 7 g of sample was brought into 70 mL sterile tap water. The sample was sonicated for 2 min, after which the supernatant was separated in a sterile flask. Again 70 mL sterile tap water was added to the struvite and sonicated. These steps were repeated for 6 times in total. The collected supernatant was used for all microbiological analyses. SSRC was determined according NEN 6567 and F-specific RNA bacteriophages according ISO 10705 part 1, coliform bacteria, *E. coli* and *Enterococcaceae* were determined according NEN-EN-ISO 9308 part 1 and NEN-EN-ISO 7899 part 2, respectively, after membrane filtration.

2.4. Struvite P availability in soil-maize seedling pot tests

Phosphorus availability from struvite was measured in pot experiments with maize seedlings for eight struvite samples (Table 1). Controls with 12.9% (P) rock phosphate (RP) and 6.9% (P) Single Super Phosphate (SSP) and a negative control with no additional P were prepared in three pots (12 × 12 × 12 cm) with 1200 g of a natural loamy-clayey soil (soil 8) with low available P (0.009 g/kg P, Olsen) and pH 5.8. To exclude effects of different granule sizes, fertilizers and struvite samples were ground to a powder and added to the soil to contain 0.017 g P/kg soil. Soils were vigorously mixed, transferred to pots and in each center a maize seed (*Zea mays* L. cv. 'Dulcano') was placed at 2.5 cm depth. Each pot was ameliorated with 0.16 g $(NH_4)_2SO_4$ -N/kg soil and 0.33 g -K_2SO_4 -K/kg soil dissolved in 50 mL of a tap water. Pots were kept in a glass house under a 16 h light/8 h dark regime,

Table 1
Overview of analyzed struvite samples. Information on process/technology, origin, recovery category (see Fig. 1: type I, II and III) and operational parameters are given, while samples are indicated that were analyzed for microbiology and used in maize seedling tests. '–': Unknown. HHNK - Hoogheemraadschap Hollands Noorderkwartier, FBR – Fluidized bed reactor, CSTR – Continuously stirred tank reactor, (A full list of all currently known European struvite installations, including production volumes, is given in Table S3, SM).

#	Process name (Technology provider)	Short name	Struvite reactor location	Country	Type of waste stream treated	Method of pH control; Mg source	Reactor type	pH	Mg:P molar ratio	P influent concentration (mg P/L)	Maximal P recovery efficiency (%)	Microbiology analyzed	Used in plant tests
1	Phosphogreen (SUEZ)	Phosgreen 1	Aby	DK	Dewatering liquor of WAS digestate + P-rich thickening liquor (type II)	Airlift for CO_2 stripping; $MgCl_2$	FBR (upflow and aerated)	7.5–8	1.2–1.8	35–100	99		
2		Phosgreen 2	Henring	DK					1.2–1.9	35–100	99	x	
3		Phosgreen 3	Marselisborg (Aarhus)	DK					1.2–1.7	35–100	99		x
4	Airprex (Centrisys/CNP)	Airprex 1	Amsterdam	NL	Digestate (type I)	$MgCl_2$	Airlift reactor	7.6–7.8	1.8–2.2	125–190	99	x	x
5a; 5b		Airprex 2 + 3	Berlin (2 samples**)	DE		$MgCl_2$		7.8–8		110	95		
6		Airprex 4	Salzgitter	DE		$MgCl_2$		8	2	280–310	97		
7		Airprex 5	Wolfsburg	DE		$MgCl_2$		–	1.2	370	97		
8	NuReSys (NuReSys)	NuReSys 2	Apeldoorn	NL	Dewatering liquor of WAS digestate (type II)	Air stripping + NaOH; $MgCl_2$	CSTR	8–8.5	1–1.1	100–140	96		x
9		NuReSys 3	Haps	NL	Dewatering liquor of WAS digestate (type II)					450–650	86		
10		NuReSys 1	Leuven	BE	Digestate (type I)					–	86		x
11		NuReSys 4	Nieuwkerke	BE	UASB effluent (type III)					120–220	90	x	x
12		NuReSys 5	Harelbeke	BE	UASB effluent (type III)					80–120	88		
13		Anphos 1	Haps (Land van Cuijk; full scale pilot)	NL	Dewatering liquor of WAS digestate (type II)	Air stripping; $Mg(OH)_2$	Tank aerated (batch)	8.8		300–700	93		x
14	Anphos + UPhos [Anphos 5 only] (Colsen)	Anphos 4	Kruiningen	NL	UASB effluent (type III)	Air stripping; MgO	Tank mixed (batch)	8.7	1–1.3	50	80		
15*		Anphos 3	Bergen op zoom	NL	UASB effluent (type III)	Air stripping; $Mg(OH)_2$		8.6–8.9		75	60		
16*		Anphos 2	's-Hertogenbosch	NL	Centrate (type II)	$Mg(OH)_2$		8.4–8.6		400	98		
17*		Anphos 5	Verrebroek (Pilot)	NL	UASB effluent (type III)	NaOH; $MgCl_2$	FBR	8.3		60–100	91		
18	Phospaq (PAQUES)	Phospaq	Olburgen	NL	UASB effluent (type III) + Dewatering liquor of WAS digestate (type II)	Air stripping; MgO	Tank aerated (continuous)	8–8.5	< 1	78	82		x
19	PEARL (Ostara)	Pearl 1	Amersfoort	NL	Dewatering liquor of WAS digestate (71%) + P-rich thickening liquor after WASSTRIP (29%) (type II)	NaOH; $MgCl_2$	FBR	7.6–7.9	Variable	200–270	83	x	x
20		Pearl 2	Slough	UK	Dewatering liquor of WAS digestate (type II)			7.7–8.1	1	100	80		
21		Pearl 3	Madrid	ES	Dewatering liquor of WAS digestate (type II)			7.8–8.0	1	130–200	80		
22	Naskeo (Naskeo)	Naskeo	Castres	FR	–	–	–	–	–	–	–		
23	Vechtstromen (Vechtstromen)	Vecht	Emmen	NL	Digestate (type I)	MgOH	CSTR	–	–	–	–		
24	HHNK (HHNK)	HHNK	Beverwijk	NL	Digestate (type I)	$MgCl_2$	CSTR	7	1.5–2	300–400	99		

* Wet struvite samples (slurry) were obtained, and were dried before analysis at 40 °C.
** 2 samples acquired at different time points.

Table 2
Estimated amount of struvite produced in 2020 in the European Union (including plants with anticipated commissioning in 2020; *excluding sample that did not meet legal requirements).

Item	Min	Max
Total struvite (t struvite /year]	9784	12,057
Total P equivalent [t P /year]	1095	1353
P equivalent of plants meeting legal limits [t P /year]	996	1254
Municipal struvite [t P /year]*	698	956
Municipal struvite [%]*	64%	71%
Potato struvite [t P /year]*	272	370
Potato struvite [%]*	25%	27%
total Anphos, Nuresys and Airprex [%]*	68%	74%
NL [%]*	35%	43%
DE [%]	15%	15%
BE [%]	16%	20%
Sum of NL, DE, BE [%]*	69%	74%

and temperatures between 19 °C (night) and 28 °C (day). Plants were regularly watered (max 200 mL), ensuring full adsorption by the soil. Soil samples for P analysis in diffusive gradients in thin films (DGT) were taken from each pot (six replicates in total) at 1, 3, 7, 14 and 28 days after germination. Soil samples were taken at the distance of 2 cm from the seed/plant using a 50 mL tube, which was pressed into the soil to the depth of 5 cm. The retrieved soil column was mixed, and 5 g soil were analyzed after drying at 37 °C for 24 h. Diffusive gels (polyacrylamide hydrogel) and the binding layer with ferrihydrite precipitated into a thin diffusive gel (ferrihydrite gel) were prepared according to Zhang and Davison (1995) and Santner et al. (2010), respectively. Soil paste of all samples with 90% water holding capacity (WHC) was placed on the DGT gels for 24 h under water-saturated air at 20 °C. After removing soils, P from gels were eluted with 2 mL 0.25 M H_2SO_4 in 3 h and P was determined in the eluate with the molybdenum blue method and determined spectrophotometrically (Estefan et al., 2013). Data points were subdued to two-way ANOVA analyses followed by Tukey Honest Significant Difference Comparisons (adjusted p values <0.01). Maize biomass was determined after 28 days, by cutting all maize stems at the position where root outgrow starts, followed by drying for 48 h at 55 °C. Data were analyzed by ANOVA and Tukey Honest Significant Difference Comparison (adjusted p values <0.01).

3. Results

3.1. Struvite installations and production volumes in Europe

In the present study 24 of a total of 39 identified operational European struvite installations were sampled, accounting together for between 59 and 67% of the struvite produced (excluding plants not operational at the time of the fieldwork but those to be commissioned in 2020, and those not separating struvite from solids, for details on methodology see SM Section 4 and Table S2). The installations identified include 29 municipal WWTP, 9 potato industry WWTP and one dairy WWTP. At these plants, 8835–11,100 tons of struvite are produced annually (Table 2), constituting an equivalent of about 1030–1350 tons P in total and between 1000 and 1250 tons struvite P that meets the legal requirement (i.e. excluding three sample as show in Section 3.2; for details on methodology see SM Section 4 and Table S2). Between 64 and 71% of struvite is recovered from municipal wastewater and 25–27% from potato wastewater. In Europe, the struvite market is currently dominated by the technologies of Airprex, NuReSys and Anphos, which are anticipated to produce 68–74% of the struvite in 2020 (including plants that do not separate struvite from sludge for Airprex). Most of the struvite is produced in the Netherlands (35–43%), Belgium (16–20%) and Germany (15%).

3.2. Struvite quality

3.2.1. Struvite constituents (P, N, Mg, K) and organic carbon

Current legislation prescribes a minimum P content within the precipitated phosphate salt of 7% DW (EC, 2019). Only one sample does not comply with this limit (Anphos 3), while 12 out of 25 samples deviate not more than 3% from the theoretical value of 12.6% P DW (Fig. 2). The source of struvite influences the P content. Struvite recovered from the dewatering liquor of digestate (type II) contains more P with a mean of 12.1% DW (standard error of mean (SEM): 0.29), while digestate has a lower P content with a mean of 11.3% (SEM: 0.24). Struvite from UASB effluent has a mean value of 10.2%, but it shows large variability (5.6–12.9%; SEM: 1.14). The NuReSys 4 and 5 samples as well as the Anphos 5 sample show high P content of >12.3%, while the Phospaq and Anphos 4 samples only show values of 8.6% and 7.3%, respectively.

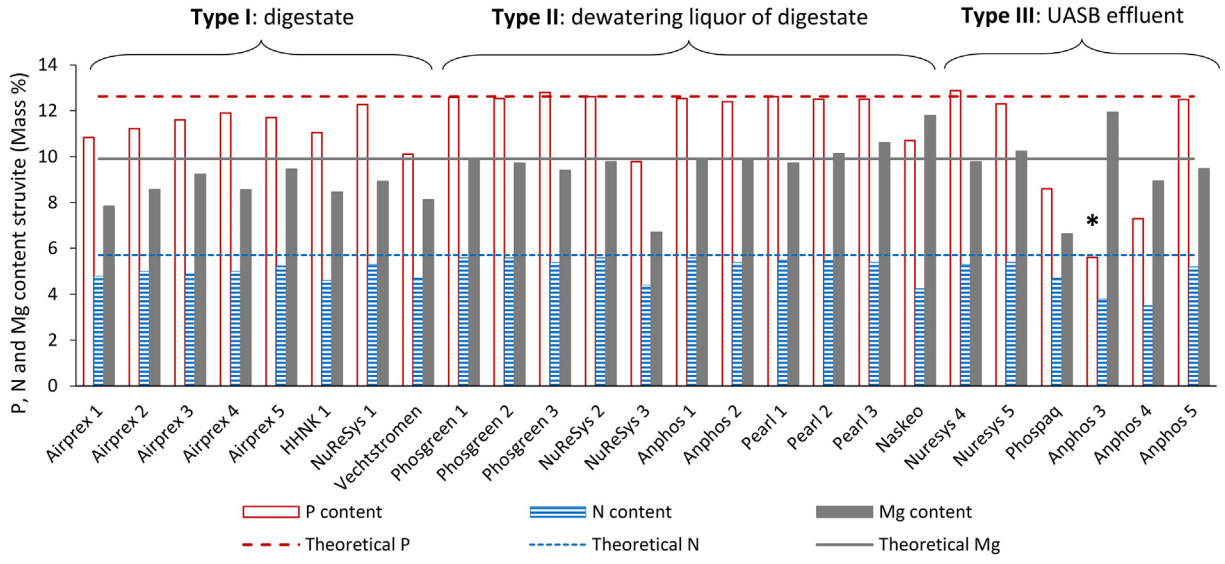

Fig. 2. Phosphorus (P), Nitrogen (N) and Magnesium (Mg) content of the analyzed struvite samples as mass % DW, recovered from the digestate (type I), from dewatering liquor of digestate (type II) and from UASB effluent (type III). The theoretical values (12.6 mass % P; 5.7 mass % N; 9.9 mass % Mg) are indicated by the lines (P: dotted red line; N: full blue line; Mg: striped grey line; * samples below the legal limit of 7 mass % for P contents within a precipitated phosphate salt).

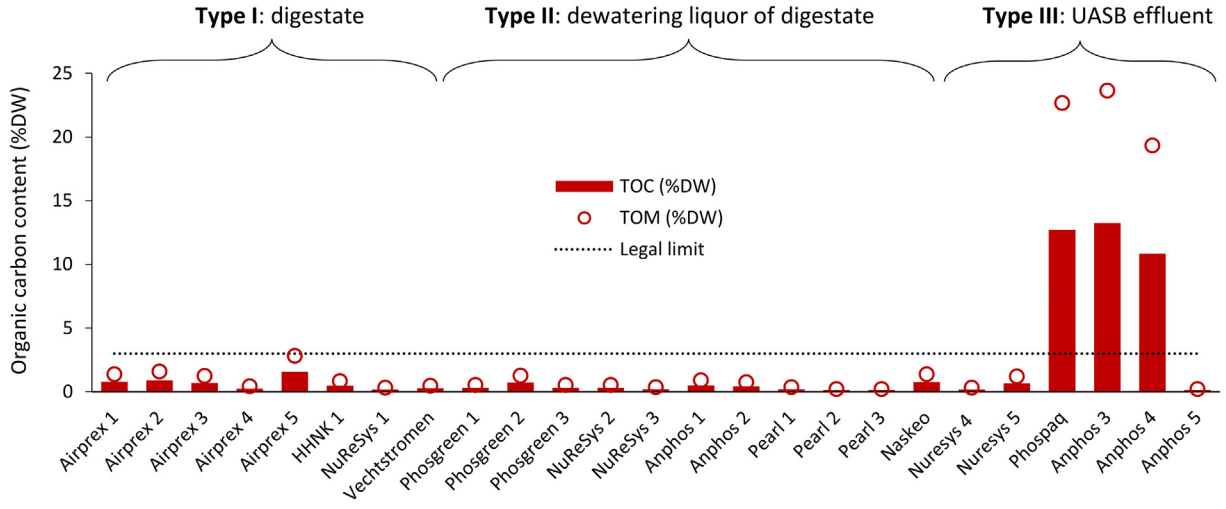

Fig. 3. Total organic carbon (TOC), and total organic matter (TOM) content, for all struvite samples. TOM was calculated as TOC/0.56. Dotted line represents the legal limit of 3% DW.

Nearly all struvite samples that have a P content close to the theoretical value also contain N and Mg close to the theoretical value of 5.7% N and 9.8% Mg (DW) (Fig. 2) (Phosphgreen 1, 2 and 3; Pearl 1, 2 and 3; NuReSys 2, 3, 4 and 5; Anphos 1, 2 and 5). For potassium (K), samples from municipal wastewater treatment show values <0.2% DW (Fig. 4), whereas all struvite samples that originate from UASB effluent (type III) show at least a 4.5 times higher K content (0.9–1.25% DW).

Of the 25 samples, 22 have a total organic carbon (TOC) content below the legal limit of 3% DW (Fig. 3), with values between 0.12 and 1.6% DW. Highest values were observed for struvite recovered from UASB effluent (10.8–13.2% DW TOC for Phospaq, Anphos 3 and 4).

3.2.2. Heavy metal content

Struvite heavy metal concentrations are well below the legal limit and often even below the detection limit (Table 3). It is suggested that heavy metal contamination can be linked to total organic matter (TOM) content (Huygens et al., 2017). This can be confirmed for the samples Phospaq, Anphos 3 and 4. However, not all the analyzed samples follow this trend, as e.g. Airprex 1 and NuReSys 3 are low in organic carbon, but high in Zn, Pb and Cu content (latter two Airprex 1 only), compared to the other samples. Struvite originating from the dewatering liquor of digestate (type II), generally shows the lowest heavy metal concentrations. Whereas samples from type I have higher heavy metal concentrations, here Zn and Cu concentrations are up to an order of magnitude higher than in most type II samples. The heavy metal content of Type III samples varies widely, with, for example, Zn concentration ranging from 2.1 to 550 mg/kg.

3.2.3. Elemental and mineralogical composition

Based on the elemental analysis, the mass balances indicate that for 19 of the 25 samples, the struvite content (i.e. magnesium ammonium phosphate) is higher than 80% DW (six samples below this value). In contrast, the mineralogical results reveal that 10 samples are below this value (Fig. 4). Based on mineralogical data, 6 samples show a struvite content between 80 and 90% DW, while 13 samples have a struvite content of >90% DW. Samples with a lower struvite content often contain elevated amounts of quartz (SiO_2), which is an important fraction of sand. Seven out of eight quartz containing samples are

Table 3
Heavy metal content of the analyzed struvite samples (Empty cells: measured content < limit of detection (LOD). N.A.: Not Applicable). Color fill of the cells indicates to which extend the regulatory limit is approached or if no regulation applies.

			Type I: digestate								Type II: dewatering liquor of digestate											Type III: UASB effluent						
Regulated metals (mg/kg)*	EU Fertilizer limit	LOD	Aiirprex 1	Aiirprex 2	Aiirprex 3	Aiirprex 4	Aiirprex 5	HHNK 1	NuReSys 1	Vecht	Phosgreen 1	Phosgreen 2	Phosgreen 3	NuReSys 2	NuReSys 3	Anphos 1	Anphos 2	Pearl 1	Pearl 2	Pearl 3	Naskeo	Nuresys 4	Nuresys 5	Phospaq	Anphos 3	Anphos 4	Anphos 5
Zn	1500	1	50	24	40	26	33	2	13	33		4.2	1.6	1.8	55		5.6	1.4			13	8.1	14	548	241	501	4.8
Cu	600	1	28	17	16	7.4	7.5	2	3.3	20					64		1.5				6.3	1.2	1.4	70	73	92	
Ni	100	1	2.3	3.4	1.5	1.4	1.1			1.3					4						12			5.5	6	5.2	
Cr VI	2	1.5																									
Cd	60	1																							1.9	2	
Pb	120	2	19	2.4	3.4	3.4				3.5					9.9									3.7	3.1	2.2	
Hg	1	0			0		0.1			0					0						0						
As (inorg.)	40	0.5	0.6												0.6						5.7			1.3	1	1.2	
Metals not regulated for in the fertilizer regulation (mg/kg)																											
Mn	N.A.	1	179	129				30	193		43	64	94	28	441	28	688	211				121		201			154
Cr	N.A.	1	2.9	1.6	3.3	4.8	2	6.2	7	2.5				6.8	13						2.7	7.5		9	5.4	5.7	

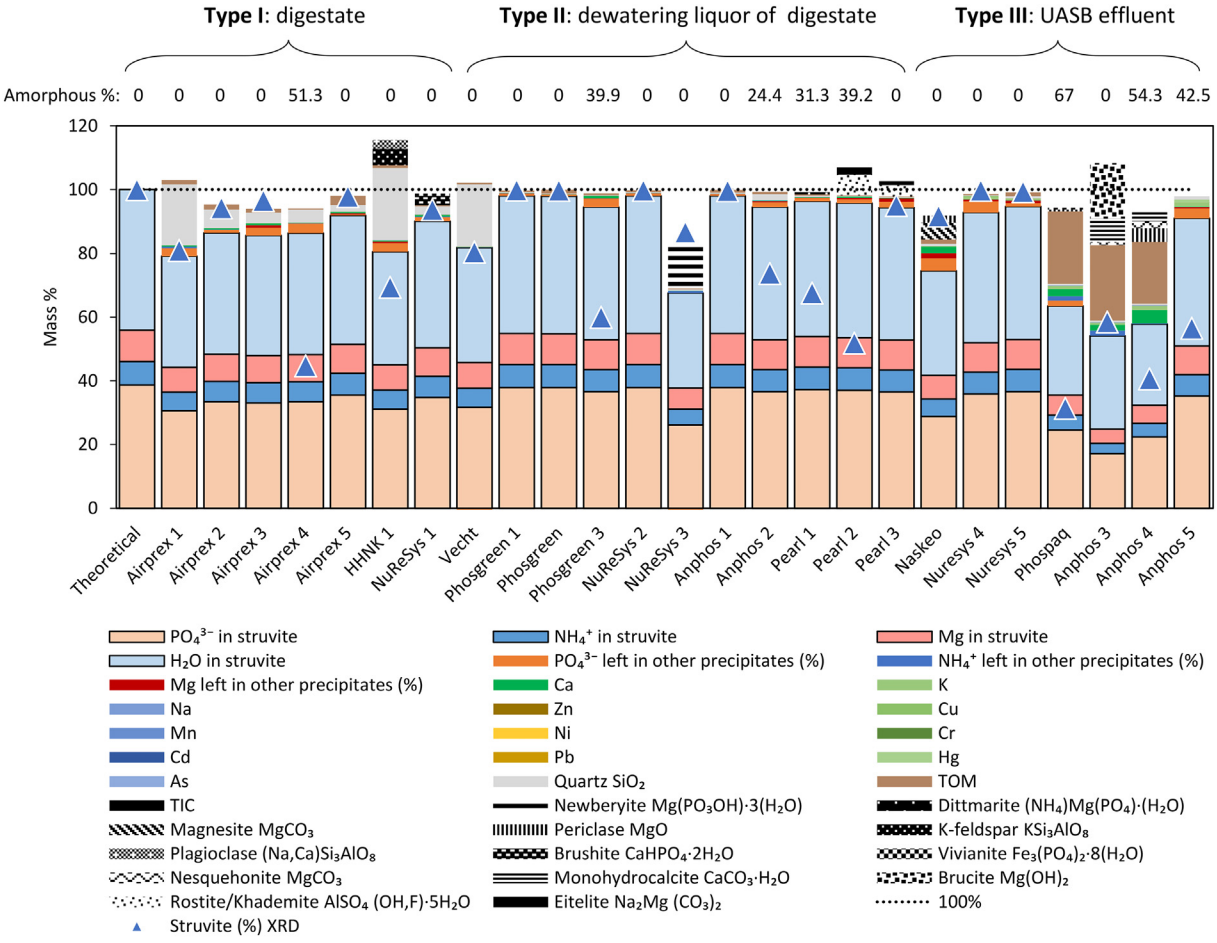

Fig. 4. Mass balance based on elemental and mineralogical data for the analyzed struvite samples. Total metal fractionation is presented in Table 3. XRD data are presented in Supplementary Material Fig. S4, raw data presented in SM Table 4.

produced on digestate (type I) (i.e. Airprex 1, 2, 3, 4 and 5; Nuresys 1 and HHNK 1 and Vecht). Furthermore, a P, N and Mg content close to the theoretical composition of struvite, does not guarantee a high struvite content, as in six samples (Phosgreen 3; Phospaq; Pearl 1, 2; Airprex 4; Anphos 4) a large fraction of amorphous phase is observed. Minerals containing Mg include periclase (3 samples), newberyte (1 sample), dittmarite (1 sample), eitelite (2 samples), nesquehonite (2 Samples) and magnesite (1 sample). Minerals containing Ca are not frequently encountered, only two samples contained monohydrocalcite in small amounts (Anphos 3: 7.4%; Anphos 4: 3.4%) and one sample contained brushite (NuReSys 1: 2.9%). Precipitates with Al are found in two samples of Pearl as rostite (Pearl 2: 6.5% and Pearl 3: 3.6%) and in the sample of HHNK (HHNK 1: 2.8%) as plagioclase. Potassium (K) was present as K-feldspar in one sample (HHNK). In other K containing samples no mineral precipitation of K could be detected. It is known that struvite can co-precipitate with K-struvite ($KMgPO_4.6H_2O$), albeit with preference for struvite because of its lower solubility (Xu et al., 2011). However, K-struvite could not be reliably be quantified as it could not be distinguished from struvite in the XRD analysis due to overlapping diffraction positions. Similarly, the integration of K-struvite into the mass balance had either almost no effect due to low K values, or was not plausible due to a lack of Mg^{2+} or PO_4^{-}in the mass balance. Therefore, while K struvite might be present (type I max 1.1%, type II max 1.2%, type III max 8.5%) a reliable quantification of its content in not possible.

3.2.4. Physical properties of struvite samples

Three struvite samples (Anphos 2, 4 and Naskeo; Fig. 5 and SM Section 6) exceed the limit for particle size distribution (PSD) of maximum 10% < 0.1 mm (note: not a legal limit defined in the revised fertilizer regulation, but proposed in an early version of the STRUBIAS working group report (Huygens et al., 2017)). Across all sampled struvite, the size range of <0.2 mm accounts for an average of 9.8% of the particles (standard error of mean (SEM): 3.9), and the majority of the particles have a size between 0.2 and 2 mm (mean: 78.5%, SEM: 6.1). Sizes above >2 mm accounted for an average of 11.7% of the particles (SEM: 4.8) (Fig. 5, SM Table S2). The largest granules are found for Anphos 5 with nearly 80% of the sample between 3.15 and 3.55 mm and Anphos 4 with 65% of the sample > 2 mm. In addition, also Phospaq contains a mass fraction of 44.5% of the sample above 2 mm. However, Anphos 3 and 4 as well as Phospaq are heterogeneous samples with no peak in the analyzed size range (Fig. 5, SM Section 6).

Investigation by struvite type shows that for digestate (type I) 81.9% of DW constitutes of granules smaller than 1 mm, while only 13.7% of the granules fall in the range of 1–2 mm and 4.4% are > 2 mm. The inverse can be found for type II, here 64.6% of the granules are between 1 and 2 mm, 33.1% of the material is <1 mm and the remainder of 2.3% is >2 mm. For type III struvite, 50.7% of the granules are smaller than 1 mm, 15.5% are between 1 and 2 mm and 33.9% are larger than 2 mm (Fig. 5, SM Table S3). The overall variability of particle sizes is highest for the type III samples, which show a distribution of grain size across the entire spectrum in many samples. Type II samples are more evenly distributed, while type I samples show the lowest variability (Fig. 5).

Visually, struvite can be classified into two types: transparent samples from digestate (type I) and opaque from the dewatering liquor of digestate and other origins (type II and III) (Fig. 5, SM Section 6). As reported also by Ping et al. (2016), we found that most struvite crystals

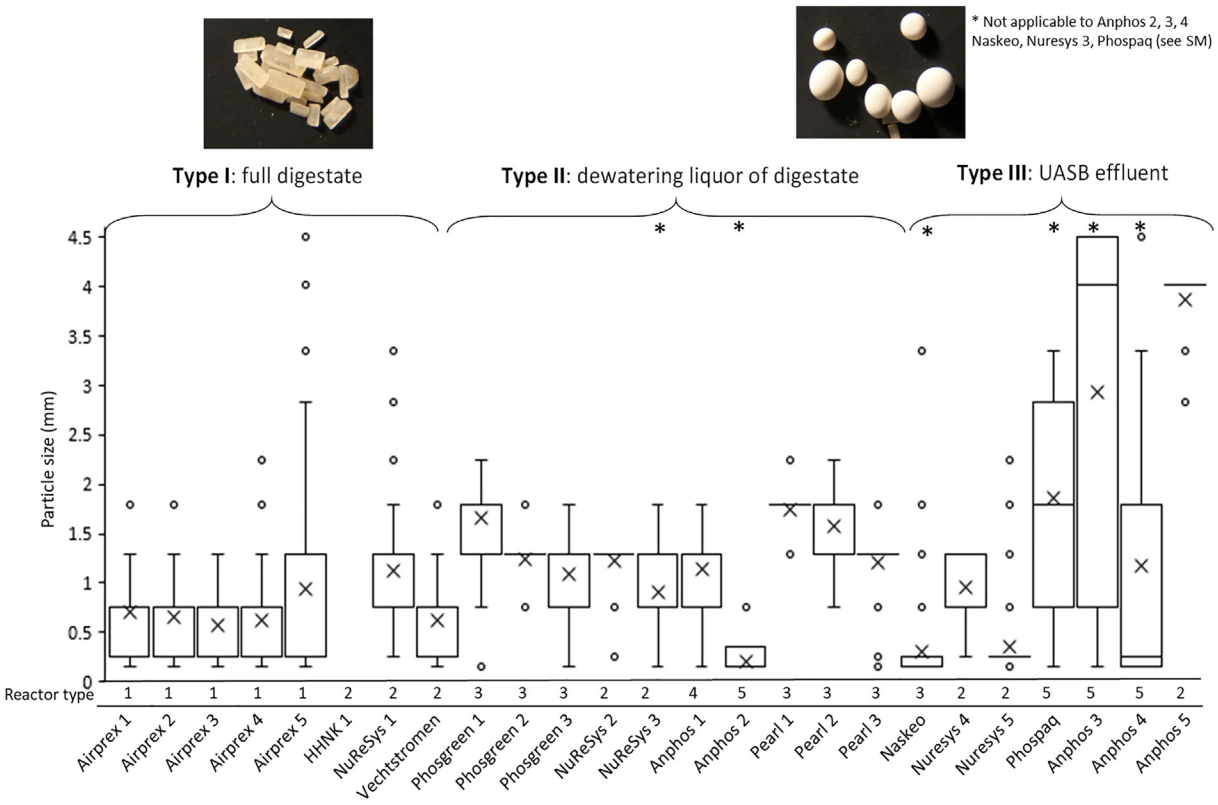

Fig. 5. Mass fraction distribution per particle size for all analyzed struvite samples. Crosses indicate the mean particle size (mm). Numbers indicate the reactor type as follows: 1 Airlift reactor, 2 Continues stirred tank reactor, 3 Fluidized bed reactor, 4 Tank aerated, 5 Tank mixed. Histograms, descriptive statistics and pictures per sample are presented in the SM Section 6, raw data shown in SM Table 4.

from the dewatering liquor of digestate or UASB effluent (type II and III) appear macroscopically (not considering <0.2 mm, i.e. Anphos 2, 3, 4, Naskeo, Nuresys 5, Phospaq – samples disintegrated easily) spherical, while crystals sourced from digestate (type I) appear more rod-shaped with pointed ends (orthorhombic shape). All struvite samples from digestate also contain visual impurities (SM Section 6).

3.2.5. Microbiological quality

Most of the pathogens and indicator organisms are present at low levels in the analyzed struvite samples. Struvite recovered from digestate (type I) contains a similar amount of Enterococcaceae (2 log cfu/g) compared to struvite recovered from dewatering liquor (type II), while struvite originating from potato processing effluent (type III) has a concentration of *Enterococcaceae* of 4 log cfu/g, violating the limit of 3 log cfu/g struvite. For SSRC the fresh samples from type I and II struvite have concentrations between 2.8 and > 4.3 log cfu/g. However, since SSRC is only a proxy indicator, this does not necessarily imply that the legal limits for the bacterium *C. perfringens* (2 log cfu/g) and *Ascaris* sp. eggs (1.4 log cfu/g) are violated.

Comparing the values for Airprex with and without impurities, it can be observed that most of the *E. coli* (>90%) and SSRC (94%) are located on the impurities, while this does not apply to the *Enterococcaceae* (30%) (Table 4). Pathogen numbers in the struvite samples of Pearl 1 and Airprex 1 are several logs lower compared to the dewatering liquor and the digestate they are produced from (Table 4). Therefore, it can be concluded that struvite crystallization selectively excludes pathogens, leaving them in the water phase or kills them off during the crystallization process (e.g. elevated pH). Furthermore, the reduction of 0.8–2.5 log units in the 9 month-stored sample of Airprex compared to the fresh sample, indicates that storage can be a good strategy to reduce pathogens.

Table 4
Pathogens and fecal indicator organisms in fresh and stored struvite samples and in struvite from digestate (type I), dewatering liquor of digestate (type II) and UASB effluent of potato wastewater (type III). *E. coli: Escherichia coli;* SSRC: spores of sulphite reducing clostridia. N.A.: Not applicable; cfu: colony-forming unit; pfu: plaque-forming unit.

			Type I: Digestate				Type II: dewatering liquor of digestate			Type III: UASB effluent
			Airprex 1				Pearl 1		Phosgreen 2	NuReSys 4
Microbial contamination	Units*	EU limits	Digestate	Struvite crystals + impurities	Struvite crystals + impurities [9 months stored]	Struvite crystals	Centrate	Struvite	Struvite [9 months stored]	Struvite
Enterococcaceae	Log cfu/g	3 (log cfu/g fresh weight)	4.5	1.6	0.8	1.9	6.3	1.5	1.2	3.7
E. coli	Log cfu/g	3 (log cfu/g fresh weight)	3.2	0.8	0	0	3	0	0	0
Coliform bacteria	Log cfu/g	N.A.	3.4	0.8	0	0	3.5	0	0	0
SSRC	Log cfu/g	N.A.	4.8	>4.3	2.8	3.1	6.9	2.5	1	1.1
F-specific RNA phages	Log pfu/g	N.A.	2.5	<0.8	<0.8	<0.8	3.6	<0.8	<0.8	<0.8

* Units are expressed per gram product (fresh weight without drying) for all samples.

3.3. Struvite P solubilization and maize plant biomass

Considering overall P availability, 7 of the 8 tested struvite samples are not significantly different from each other; while one struvite sample (Phosgreen 3) differs from at least 4 other samples by lower overall P availability (Fig. 6). It can be observed that P availability patterns are rather similar, with a continuous availability over the sample period (3.5–6.5 mg P/L of soil, mean: 4.8 mg P/L). As expected, P availability from SSP peaks at day one (9.09 mg P/L) and then declines. Starting on day seven, P availability of struvite is not significantly different from SSP (SM Table S5). Rock Phosphate (RP) P availability is significantly lower than that of struvite and increases only marginally over the sampling period. Regarding maize seedling biomass, no significant difference is observed between struvite samples and SSP fertilization (Fig. 6B). However, due to the short sampling period significant differences between soil only, SSP and RP could not be achieved. Nonetheless, the data indicates a trend towards a better performance of struvite and SSP (SM Table S6).

4. Discussion

4.1. Struvite installations and production volumes in Europe

Of the 39 operational European struvite production sites, an estimated equivalent of 1000–1250 tons P is available that meets legal requirements (Section 3.1). This corresponds to 0.5% of the total P theoretically contained in EU wastewater or 0.06–0.07% of the EU P imported for fertilizer use in 2017 (estimated based on a population of 508 million in EU-28, a discharge of 1.2 g P/person/day and an import of 1.725 million ton P/year (FAO, 2020)). In other words, currently recovered amounts are very low compared to the overall P flows and the demand of agriculture. Moreover, recovery of struvite from municipal wastewater has an efficiency ($P_{struvite}$ /$P_{total\text{-}plant\text{-}influent}$) of between 20 and 43% (Amann et al., 2018; Kazadi Mbamba et al., 2016). Assuming a maximum struvite recovery efficiency of 43%, this would supply about 13% of the P-fertilizer demand in the EU.

4.2. Differences and similarities between samples

4.2.1. Elemental and mineralogical composition

This study demonstrates that 22 struvite samples have a chemical quality that is within the legal limits set by the new EU fertilizer regulation. The only legal infringements of the chemical composition can be found for the organic carbon content of three samples (Phospaq, Anphos 3, 4), of which one also failed the minimum required P content (Anphos 3). Another observation is that eight samples contain relatively high amounts of amorphous precipitates. Amorphous calcium phosphate in the crystals was described at high Ca concentrations in the solution of up to 4 mM (Le Corre et al., 2005; Pastor et al., 2010). Furthermore, above a reactor pH of 9.5, it was found that the struvite content decreased to <30% and amorphous P precipitates increased. In addition, it was observed that struvite crystal structure changes at temperatures above 64 °C (Doyle et al., 2002), potentially increasing the number of amorphous components. However, none of these reasons can consistently be aligned with our findings. The samples that contain the highest amount of Ca also contain amorphous substances (Anphos

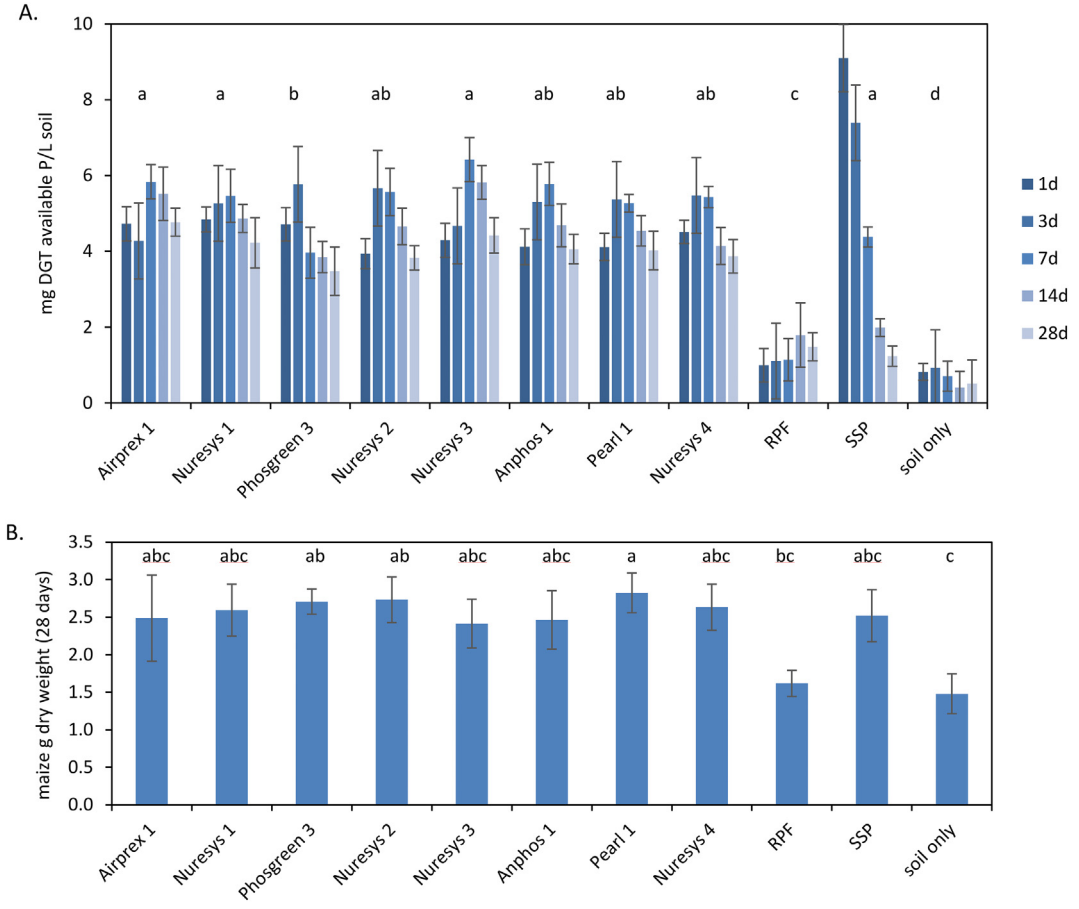

Fig. 6. A) Available P in days after germination in maize seedlings pots fertilized with struvite, rock phosphate (RP), single super phosphate (SSP) or without additional P fertilization (soil only). P collected in 24 h hours with DGT after the indicated time points are shown. P application was normalized to the P content of each sample so that in each pot the same amount of P was applied. B) Maize seedling dry weight after 28 days. Letter codes indicate significant differences between overall release patterns (i.e. different letters represent significant differences $p < 0.01$), for example letter combinations containing the latter 'a' are not significantly different from each other, while a combination not containing the letter 'a' is significantly different.

4, Phospaq), but other samples with a similar Ca-content do not contain amorphous substances (Naskeo, Anphos 3). For the Pearl and the Phosgreen processes, struvite is heated (40–55 and 55–75 °C, respectively), but not all of these processes show amorphous components. Values for the pH were generally well below 9.5 in the reactors.

Another observation is that type III struvite has a 4.5 times higher K content than other struvite types, which is likely a result of the higher K content in the potato wastewater (around 1800 mg K/L), compared to municipal wastewater (10–30 mg K/L) (Arienzo et al., 2009). Similarly, quartz is abundant in the type I digestate. The quartz content is relatively high for these samples as in the other processes it is removed in the solid-liquid separation that is preceding the struvite reactor. Furthermore, it was found that there is a tendency towards a higher heavy metal content for type I struvite. Heavy metals are known to attach to organic matter, however, no correlation between heavy metal content and TOC was found in the struvite of type I. Nonetheless, it is plausible that struvite precipitated from a matrix that contains comparative high concentrations of organic matter would show higher values of heavy metals.

4.2.2. Physical properties

The particle sizes ranged from <0.2 to >4.5 mm, therefore larger samples (Anphos 5 only) were found in this research than previously described in literature (i.e. 0.15 mm (Zhang et al., 2009) to 3.5 mm (Adnan et al., 2003)). Granules from the dewatering liquor of digestate are generally larger than those from digestate (type I). This may be explained by the higher TSS concentration in the struvite reactors of type I operating on digestate (25 ± 5 g TSS/L (Airprex 1) compared to dewatering liquor (1 ± 0.1 g TSS/L (Pearl 1). Ping et al. (2016) found that at elevated TSS concentrations, struvite crystals are smaller. They suggest that TSS interferes with the crystal growth by reducing the aggregation (i.e. the collision of two crystals and their adherence together) of crystals. The TSS content in UASB effluent is comparatively low (0.5 g TSS/L (Muys et al., 2020)) and should not prevent crystal aggregation for type III struvite. In fact, the largest struvite granules were found for this type of struvite, but the variability in size distribution was highest for these sample, ranging from <0.2 mm to >4.5 mm. Likely, complex interactions between other determining parameters play a role here including: agitation, crystal residence time, presence of foreign ions, pH as well as the Mg:P ratio. However, due to the interactions of different parameters and the limited availability, reliable conclusions about the effect of these processes on particle size cannot be made.

In addition to the crystal size, the visual difference between the shape and appearance (i.e. transparent and opaque) of type I, II and III were observed (Fig. 5). An explanation for the differences comes from Ye et al. (2018), they describe an evolution of crystal shapes in a fluidized bed reactor, from a primary nucleus followed by crystal growth to 'young' rod-shaped crystals and subsequent aggregation of individual crystals. This is further followed by agglomeration or the formation of clusters of aggregates in the middle section of the fluidized bed. Finally, clusters sink to the bottom of the fluidized bed where they are coated with primary crystallization nuclei (i.e. crystal coalescence). Throughout this evolution, crystals become more spherical with a smoother surface. As this study observed spherical struvite granules with a smoother surface from fluidized bed reactors, CSTRs and aerated tanks, it could be possible that, independent of the reactor type, similar processes as described by Ye et al. (2018) take place. This appears plausible as every type of agitation will create a fluidized bed of solid particles. However, the conclusion about the particle character should be first validated by providing a transect of struvite granules as done by Ye et al. (2018). With exceptions (i.e. samples mainly <0.2 mm), Type II and III would then correspond to agglomerated clusters and coated granules.

Ye et al.'s (2018) classification could also suggest that type I struvite comprises crystals which may be unable to agglomerate or break apart easily once agglomerated as suggested by Ping et al. (2016). According to Ping et al. (2016) the reason for this attrition lies in the elevated TSS concentrations, which also has been observed in other studies (Tarragó et al., 2018; Ye et al., 2018). Another indication for reduced agglomeration has been associated to the lower viscosity of influent that contains a higher faction of colloidal substances. Colloids slow down the reaction kinetics and result in the formation of fewer agglomerated crystals (Capdevielle et al., 2016).

4.2.3. Biological properties

Struvite contamination with *Enterococcaceae*, *E. coli*, Coliform bacteria and F-specific RNA phages is low compared to the regulatory requirements and the influent they are produced from. Specially, for phages it has been described that they are mainly contained in the water phase and that adsorption to struvite granules does not occur (Decrey et al., 2011). It has been suggested that adsorption cannot occur because struvite, in a struvite saturated solution, is charged positive and, as phages are also positively charged, this is leading to electrostatic repulsion (Decrey et al., 2011). SSRC as a proxy indicator for *Ascris* eggs and *Clostridium perfringens* are of concern as their number exceeds the legal limits for these pathogens. Furthermore, the elevated SSRC level may indicated a low *Cryptospridium* oocyst removal efficacy. However, as SSRC are only a proxy indicator, reliable statements about removal and viability of these pathogens cannot be drawn from this study. In addition to pathogen removal in the struvite production process, it was observed that storage is a good strategy to reduce pathogen contamination. A similar observation was made by Decrey et al. (2011). These authors detected a 0.07 log reduction/d at 20 °C/93% relative humidity for phages and observed a comparatively low reduction of activity of 0.003–0.01 log after three days at storage at 20 °C for *Ascaris* eggs. In the present research, a higher reduction of 0.08 log of the proxy indicator SSRC in three days can be calculated (assuming a linear reduction over a nine months period). Since struvite recovered from digestate (type I) contained more pathogens compared to struvite from the dewatering liquor of digestate (type II), this type of struvite should be monitored more closely. The reasons for the elevated *Enterococcaceae* count in struvite originating from potato processing effluent should be explored. For SSRC, determination of *C. perfringens* should be performed to shed light on the actual risk, as this was not feasible in this research. After hand-picking macroscopic impurities and struvite washing, a significantly lower number of pathogens was observed by Huygens et al. (2017). The positive effect of hand-picking impurities on pathogen contamination was also confirmed in this study. Finally, heating struvite to temperatures just above 35 °C or a temperature at which it is expected that crystalline structure of struvite is not yet changing, showed to be an effective way to reduce the numbers of viable pathogens including *Ascaris* eggs and phages in struvite (Decrey et al., 2011). Therefore, a gentle drying process may further reduce pathogen contamination.

4.3. Fertilizers use

4.3.1. P availability and growth performance

The results showed that despite differences in the mineralogical composition of struvite, there is no significant difference between samples in terms of plant yields. Similarly, for all struvite samples a continuous P availability over the sample period was detected, indicating the often described 'slow release' character of struvite. In literature, a more heterogeneous release of different struvite types has been described. Rech et al. (2019) tested three different struvite samples and observed a P availability of 234–261 mg P/L on day one, for a laboratory sample originating from chicken manure (this sample contained more K than in any of the samples observed and contained only 7.6% P). This sample showed a P availability pattern similar to that of SSP and Triple Super Phosphate (TSP), with a high availability at the start and a continued decline. For the other two samples, Rech et al. (2019) found P availabilities comparable to the present study: mean 4.75 ± 0.68 mg P/L; this study 4.8 ± 0.5 mg P/L. Moreover, Rech et al. (2019) found that TSP and the conventional struvite obtained the same P availability after 17 days.

In the present study, this point was reached at day 7 when compared with SSP. The earlier occurrence of the point is likely a result of the more than two times higher P content of TSP as compared to SSP (i.e. 6.9% (P) in the present study and 19.35–21% (P) TSP in the study of Rech et al. (2019). Literature indicates that these slow release characteristics can reduce P loss and the associated environmental impact (Everaert et al., 2018; Hertzberger et al., 2020).

4.3.2. Physical properties and fertilizer processing

The physical properties of struvite are of relevance to enable its agronomic use. Struvite granules must be of a shape and size which enable its utilization in modern application equipment. Small granules 1–2.5 mm are used for applications in rows, macro granules 2–3.5 mm are used for spreading and smaller granules may be used for specialized applications such as growth media (Grunert et al., 2019). Furthermore, there is also a market demand for component fertilizers that are containing N-P-K in suitable ratios. If struvite is to be used in N-P-K fertilizers, the P contained in struvite must either be incorporated into a complex granule or blended with N and K granules. Spiller et al. (2019) suggest type II struvite is most likely to be blended as it has reasonably large granules with a relatively homogenous distribution in the range between 1 and 2 mm. However, the authors also point out that the granules are still too small to blended as this is usually practiced at granules sizes between 2 and 3 mm. Whereas, type I and type III struvite is most likely to be reprocessed or used for specialized application (i.e. growing media) due to their irregular shape or small grain size. The results of this study support these conclusions but suggest that individual processes and sites provide larger and high-quality granules. This is demonstrated by the sample Anphos 5 (type III), with the majority of granules exceeding 3.5 mm. Therefore, a case by case assessment is required to determine potential struvite utilization routes.

5. Conclusion

- Up to 1250 ton of the 1350 ton struvite produced annually in the EU can be considered suitable for direct use as fertilizer or as secondary raw material for fertilizer production. Established processes in the EU produce struvite with a high quality and little variability in terms of chemical parameters. Only three struvite samples failed legal limits: one for a P content of minimal 7% DW (Anphos 3) and three (Phospaq, Anphos 3, Anphos 4) for an organic carbon content exceeding 3% of DW.
- Current replacement of fertilizer P imports to the EU by struvite account for 0.5%. The theoretical maximum replacement is estimated to be 13% of fertilizer P imports.
- The research demonstrated a rather uniform P availability of between 3.5 and 6.5 mg P/ kg soil per day over the experimental period.
- It is suggested that struvite from different origins may be utilized in different application routes. Type II and III may be suitable for blending into N-P-K fertilizers due to their spherical shape, while type I struvite is more suited to be utilized for other applications (e.g. in growing media).
- Analysis of the biological contamination of struvite indicates that struvite may exceed certain legal limits (e.g. *Ascaris eggs, Clostridium perfringens based on SSRC as proxy*), but also, that storage or removal of impurities can reduce contamination. However, at this point no conclusions about biological contamination and mitigation can be made since a more detailed analysis of biological parameters is necessary.

Supplementary data to this article can be found online at https://doi.org/10.1016/j.scitotenv.2020.143726.

CRediT authorship contribution statement

Maarten Muys: Methodology, Formal analysis, Writing - original draft, Data curation. **Rishav Phukan:** Data curation. **Günter Brader:** Formal analysis, Resources. **Abdul Samad:** Formal analysis, Resources. **Michele Moretti:** Writing - review & editing. **Barbara Haiden:** Data curation. **Sylvain Pluchon:** Formal analysis, Resources. **Kees Roest:** Formal analysis. **Siegfried E. Vlaeminck:** Writing - review & editing, Funding acquisition. **Marc Spiller:** Conceptualization, Formal analysis, Funding acquisition, Supervision, Writing - review & editing.

Declaration of competing interest

The authors declare that they have no known competing financial interests or personal relationships that could have appeared to influence the work reported in this paper.

Acknowledgements

The SUSFERT project has received funding from the Bio-Based Industries Joint Undertaking (BBI-JU) under the European Union's Horizon 2020 research and innovation program under grant agreement No. 792021. The author would also like to thank everyone that supplied struvite samples and/or information as an input to this study.

References

Abma, W.R., Driessen, W., Haarhuis, R., MCM, Van Loosdrecht, 2010. Upgrading of sewage treatment plant by sustainable and cost-effective separate treatment of industrial wastewater. 61, 1715.
Adnan, A., Koch, F.A., Mavinic, D.S., 2003. Pilot-scale study of phosphorus recovery through struvite crystallization – II: applying in-reactor supersaturation ratio as a process control parameter. J. Environ. Eng. Sci. 2, 473–483.
Amann, A., Zoboli, O., Krampe, J., Rechberger, H., Zessner, M., Egle, L., 2018. Environmental impacts of phosphorus recovery from municipal wastewater. Resour. Conserv. Recycl. 130, 127–139.
APHA, AWWA, WEF, 2012. Standard Methods for the Examination of Water and Wastewater. American Public Health Association.
Arienzo, M., Christen, E.W., Quayle, W., Kumar, A., 2009. A review of the fate of potassium in the soil-plant system after land application of wastewaters. J. Hazard. Mater. 164, 415–422.
Capdevielle, A., Sýkorová, E., Béline, F., Daumer, M.-L., 2016. Effects of organic matter on crystallization of struvite in biologically treated swine wastewater. Environ. Technol. 37, 880–892.
Chowdhury, R.B., Moore, G.A., Weatherley, A.J., Arora, M., 2017. Key sustainability challenges for the global phosphorus resource, their implications for global food security, and options for mitigation. J. Clean. Prod. 140, 945–963.
De Vrieze, J., Colica, G., Pintucci, C., Sarli, J., Pedizzi, C., Willeghems, G., et al., 2019. Resource recovery from pig manure via an integrated approach: a technical and economic assessment for full-scale applications. Bioresour. Technol. 272, 582–593.
Decrey, L., Udert, K.M., Tilley, E., Pecson, B.M., Kohn, T., 2011. Fate of the pathogen indicators phage ΦX174 and Ascaris suum eggs during the production of struvite fertilizer from source-separated urine. 45, 4960–4972.
Doyle, J.D., Parsons, S.A., 2002. Struvite formation, control and recovery. Water Res. 36, 3925–3940.
Doyle, J.D., Oldring, K., Churchley, J., Parsons, S.A., 2002. Struvite formation and the fouling propensity of different materials. Water Res. 36, 3971–3978.
EC, 2003. Regulation (EC) no 2003/2003 of the European Parliament and of the council of 13 October 2003 relating to fertilisers parliament E. https://eur-lex.europa.eu/legal-content/GA/TXT/?uri=CELEX:32003R2003:.
EC, 2019. Regulation (EU) 2019/1009 of the European Parliament and of the council of 5 June 2019 laying down rules on the making available on the market of EU fertilising products and amending regulations (EC) no 1069/2009 and (EC) no 1107/2009 and repealing regulation (EC) no 2003/2003 (text with EEA relevance). European Parliament. https://eur-lex.europa.eu/legal-content/EN/TXT/?uri=CELEX%3A32019R1009:.
EC, 2020. Critical raw materials. https://ec.europa.eu/growth/sectors/raw-materials/specific-interest/critical_en:2020 27/10.
Egle, L., Rechberger, H., Krampe, J., Zessner, M., 2016. Phosphorus recovery from municipal wastewater: an integrated comparative technological, environmental and economic assessment of P recovery technologies. Sci. Total Environ. 571, 522–542.
Estefan, G., Sommer, R., Ryan, J., 2013. Methods of Soil, Plant, and Water Analysis: A Manual for the West Asia and North Africa Region: International Center for Agricultural Research in the Dry Areas.
Everaert, M., Da Silva, R.C., Degryse, F., McLaughlin, M.J., Smolders, E., 2018. Limited dissolved phosphorus runoff losses from layered double hydroxide and struvite fertilizers in a rainfall simulation study. J. Environ. Qual. 47, 371–377.
FAO, 2020. Fertilizers by nutrient. http://www.fao.org/faostat/en/#data/RFN:2020.
Grunert, O., Robles-Aguilar, A.A., Hernandez-Sanabria, E., Schrey, S.D., Reheul, D., Van Labeke, M.-C., et al., 2019. Tomato plants rather than fertilizers drive microbial community structure in horticultural growing media. Sci. Rep. 9, 9561.
Guzman, C., Jofre, J., Montemayor, M., Lucena, F., 2007. Occurrence and levels of indicators and selected pathogens in different sludges and biosolids. J. Appl. Microbiol. 103, 2420–2429.

Hertzberger, A.J., Cusick, R.D., Margenot, A.J., 2020. A review and meta-analysis of the agricultural potential of struvite as a phosphorus fertilizer. Soil Sci. Soc. Am. J. 84 (3), 653–671.

Huygens, D., Saveyn, H., Tonini, D., Eder, P., Sancho, L.D., 2017. DRAFT STRUBIAS technical proposals – DRAFT nutrient recovery rules for recovered phosphate salts, ash-based materials and pyrolysis materials in view of their possible inclusion as component material categories in the revised Fertiliser regulation. Comission J-E. https://phosphorusplatform.eu/images/download/STRUBIAS-draft-report-24-5-17-I.pdf:.

Kazadi Mbamba, C., Flores-Alsina, X., John Batstone, D., Tait, S., 2016. Validation of a plant-wide phosphorus modelling approach with minerals precipitation in a full-scale WWTP. Water Res. 100, 169–183.

Le Corre, K.S., Valsami-Jones, E., Hobbs, P., Parsons, S.A., 2005. Impact of calcium on struvite crystal size, shape and purity. J. Cryst. Growth 283, 514–522.

Moerman, W., Carballa, M., Vandekerckhove, A., Derycke, D., Verstraete, W., 2009. Phosphate removal in agro-industry: pilot- and full-scale operational considerations of struvite crystallization. Water Res. 43, 1887–1892.

Muys, M., Papini, G., Spiller, M., Sakarika, M., Schwaiger, B., Lesueur, C., et al., 2020. Dried aerobic heterotrophic bacteria from treatment of food and beverage effluents: screening of correlations between operation parameters and microbial protein quality. Bioresour. Technol. 307, 123242.

Pastor, L., Mangin, D., Ferrer, J., Seco, A., 2010. Struvite formation from the supernatants of an anaerobic digestion pilot plant. Bioresour. Technol. 101, 118–125.

Ping, Q., Li, Y., Wu, X., Yang, L., Wang, L., 2016. Characterization of morphology and component of struvite pellets crystallized from sludge dewatering liquor: effects of total suspended solid and phosphate concentrations. J. Hazard. Mater. 310, 261–269.

Rech, I., PJA, Withers, Jones, D.L., Pavinato, P.S., 2019. Solubility, diffusion and crop uptake of phosphorus in three different Struvites. Sustainability 11.

Santner, J., Prohaska, T., Luo, J., Zhang, H., 2010. Ferrihydrite containing gel for chemical imaging of labile phosphate species in sediments and soils using diffusive gradients in thin films. Anal. Chem. 82, 7668–7674.

Shaddel, S., Bakhtiary-Davijany, H., Kabbe, C., Dadgar, F., Osterhus, S.W., 2019. Sustainable sewage sludge management: from current practices to emerging nutrient recovery technologies. Sustainability 11.

Spiller, M., Muys, M., Moretti, M., Haiden, B., Pluchon, S., Brader, G., et al., 2019. SUSFERT deliverable 1.4 to the EU: recommendations for struvite producers to make their product suitable for use as phosphorous source in fertilisers. https://www.susfert.eu/wp-content/uploads/2019/09/SUFERT_Public-Deliverable_Marc-Spiller_Struvites_UPDATE-Sept19.pdf:.

Talboys, P.J., Heppell, J., Roose, T., Healey, J.R., Jones, D.L., Withers, P.J.A., 2016. Struvite: a slow-release fertiliser for sustainable phosphorus management? Plant Soil 401, 109–123.

Tarragó, E., Sciarria, T.P., Ruscalleda, M., Colprim, J., Balaguer, M.D., Adani, F., et al., 2018. Effect of suspended solids and its role on struvite formation from digested manure. J. Chem. Technol. Biotechnol. 93, 2758–2765.

van Dijk, K.C., Lesschen, J.P., Oenema, O., 2016. Phosphorus flows and balances of the European Union member states. Sci. Total Environ. 542, 1078–1093.

Xu, K., Wang, C., Liu, H., Qian, Y., 2011. Simultaneous removal of phosphorus and potassium from synthetic urine through the precipitation of magnesium potassium phosphate hexahydrate. Chemosphere 84, 207–212.

Ye, Z.-L., Deng, Y., Ye, X., Lou, Y., Chen, S., 2018. Application of image processing on struvite recovery from swine wastewater by using the fluidized bed. Water Sci. Technol. 77, 159–166.

Zhang, H., Davison, W., 1995. Performance-characteristics of diffusion gradients in thin-films for the in-situ measurement of trace-metals in aqueous-solution. Anal. Chem. 67, 3391–3400.

Zhang, T., Ding, L., Ren, H., 2009. Pretreatment of ammonium removal from landfill leachate by chemical precipitation. J. Hazard. Mater. 166, 911–915.